Published in final edited form as:
J Med Chem. 2013 March 28; 56(6): 2665–2675. doi:10.1021/jm400079a.

Arylazanylpyrazolone derivatives as inhibitors of mutant superoxide dismutase 1-dependent protein aggregation for the treatment of amyotrophic lateral sclerosis

Yinan Zhang[1], **Radhia Benmohamed**[2], **He Huang**[1], **Tian Chen**[1], **Cindy Voisine**[3,4], **Richard I. Morimoto**[3], **Donald R. Kirsch**[2], and **Richard B. Silverman**[1,*]

[1]Department of Chemistry, Department of Molecular Biosciences, Chemistry of Life Processes Institute, Center for Molecular Innovation and Drug Discovery, Northwestern University, Evanston, Illinois 60208-3113, USA

[2]Cambria Pharmaceuticals, Cambridge, Massachusetts 02142, USA

[3]Department of Molecular Biosciences, Rice Institute for Biomedical Research, Northwestern University, Evanston, Illinois 60208-3500, USA

Abstract

The arylsulfanyl- and aryloxanylpyrazolone scaffolds previously were reported to inhibit Cu/Zn superoxide dismutase 1 dependent protein aggregation and to extend survival in the ALS mouse model. However, further evaluation of these compounds indicated weak pharmacokinetic properties and a relatively low maximum tolerated dose. On the basis of an ADME analysis, a new series of compounds, the arylazanyl pyrazolones, has been synthesized, and structure-activity relationships were determined. The SAR results showed that the pyrazolone ring is critical to cellular protection. The NMR, IR, and computational analyses suggest that phenol-type tautomers of the pyrazolone ring are the active pharmacophore with the arylazanylpyrazolone analogues. A comparison of experimental and calculated IR spectra is shown to be a valuable method to identify the predominant tautomer.

Introduction

Amyotrophic lateral sclerosis (ALS), a rapidly fatal neurodegenerative disease, is characterized by progressive loss of upper and/or lower neurons in the motor cortex, brainstem, and ventral spinal cord.[1] Although the incidence and prevalence of the disease are relatively low, compared with other neurodegenerative diseases, such as Parkinson's disease and Alzheimer's disease, it has the most rapid progression to death, in most cases within 3-5 years after diagnosis.[2] Moreover, an observed increased prevalence,[3] higher risk for military personnel,[4] and high cost for care in the late stages of ALS,[5] resulting in extreme economic and emotional burdens to the patients and their families, nearly one-third of whom reside in the United States.[6] The sole FDA-approved drug, riluzole, a presumptive anti-glutamatergic agent, extends survival by only 2-3 months.[7]

*Corresponding author Tel: 847-491-5663. Fax: 847-491-7713. Agman@chem.northwestern.edu.
[4]Current address: Department of Biology, Northeastern Illinois University, Chicago, IL 60625, USA

Supporting Information

NMR spectra for compounds **2–38**, IR spectra for compounds **30, 31**, and **38**, and primary cortical neuron protection assay for compounds **1, 3, 19, 20, 21, 23, 24**, and **27**. This material is available free of charge via the Internet at http://pubs.acs.org

Although the mechanistic basis of ALS, as well as the cause of motor neuron death, remain controversial, a cohort of susceptibility genes producing ALS have been identified from familial ALS patients,[8] such as fused in sarcoma, senataxin, TAR DNA binding protein (TDP-43), and UBQLN2. The discovery of the toxicity of mutant Cu/Zn superoxide dismutase 1 (SOD1) provides the first insight into potential causes for ALS[9] and contributes the most to our understanding of ALS pathology, which includes calcium mediated excitotoxicity, oxidative stress, mitochondrial dysfunction, and aberrant RNA processing.[10] Recent observations that mutant SOD1-expressing astrocytes are toxic to motor neurons in both familial and sporadic ALS,[11-12] together with the fact that SOD1 mediated protein misfolding and aggregation have proven to be associated with ALS pathogenesis,[13] suggest a possible therapeutic treatment involving protection against mutant SOD1-induced cytotoxicity. We, therefore, developed an assay using PC12 cells expressing G93A SOD1 [14] and carried out a high-throughput screen to identify compounds that protected these cells from protein aggregation and toxicity. [15] One of the hit scaffolds was the arylsulfanylpyrazolones (ASP), which exhibited good in vitro potency, but was rapidly metabolized.[16] The metabolic hot spot was identified as the sulfur atom, which was readily oxidized. Conversion to the corresponding ether led to much more stable compounds, and one analogue extended the life of G93A ALS mice by 13.3% at 20 mg/kg.[17] A SAR study characterized the important parts of this class of compounds.[18] In search of more potent and metabolically stable compounds, which also would allow diverse substitutions to carry out target identification studies, we synthesized the corresponding arylazanylpyrazolones (AAPs). These compounds are the focus of this paper (Figure 1).

Results and Discussion

Chemistry

Two synthetic strategies were utilized to synthesize β-ketoesters, the critical intermediate for the construction of the pyrazolone ring. As shown in Scheme 1, the upper route started from the reaction of alkyl anilines or sulfonyl amides with ethyl bromoalkanoate. The ester intermediates reacted with the enolate of ethyl acetate, providing the aniline substituted β-ketoesters in moderate to high yields. The lower single-step route was carried out using an optimized methodology[19] based on the reaction of the aniline with ethyl 4-chloroacetoacetate, resulting in a series of anilino substituted β-ketoester intermediates with varied R and R' substituents. All of the β-ketoester intermediates were transformed to pyrazolones in high yields with hydrazine.

An alternative synthetic route (Scheme 2) was designed for bulky R groups, such as t-butyl, phenyl, and benzyl, which gave low yields of anilino esters in the reaction above. By employing ethyl diazoacetate, an NH insertion occurred to achieve the anilino esters in good yields,[20] which were used to generate the β-ketoester intermediates by attack of the enolate of ethyl acetate.

The N^1-methyl pyrazolone analogue (**30**) was easily obtained by replacing hydrazine with methyl hydrazine in the heterocycle formation (Scheme 3). The N^1-methyl pyrazolones can be further modified to dimethyl- and trimethyl-substituted pyrazolone analogues (**32-34**). Although it has been reported that the condensation between methyl hydrazine and a β-ketoester produces a mixture of N^1-alkyl and N^2-alkyl isomers,[21] no N^1-alkyl product was observed with our substrate. With the help of a method developed by Janin and coworkers,[22] our attempts to synthesize the N^2-alkyl product (**31**) were successful, as shown in Scheme 3. The β-ketoester intermediate was initially converted to N^1-2-hydroxylethyl-N^2-tosyl pyrazolone derivative **35** in an 85% yield, which was then treated with sodium hydride to give key intermediate **36** containing a 2,3-dihydropyrazolo[3,2-b]oxazole ring. Alkylation with MeOTf, dihydrooxazole ring-opening with sodium iodide, followed by elimination of

hydrogen iodide, led to N^1-vinyl-N^2-methyl pyrazolone **37** in a 55% yield. Acid hydrolysis gave the desired N^1-methyl pyrazolone analogue (**31**).

In vitro activity of secondary and tertiary AAPs

Compound **1** has an oral bioavailability of 27%, PK half-life of 3.6 hours, and maximum tolerated dose of 75 mg/kg, which meet the standard minimal criteria for preclinical advancement.[23] However, some pharmacokinetic properties of **1** need improvement. For example, as indicated by the oral bioavailability,[17] the AUC/dose of **1** showed a distinct difference between i.v. (184 ng*h/mL/dose) and p.o. (50 ng*h/mL/dose) administration. Given good aqueous solubility and cell permeability, one of the most likely causes for the difference between these two routes of administration is the first-pass clearance from hepatic and gut metabolism.[24] To increase metabolic stability and further diversify the structure, the ether oxygen was replaced by the isosteric amine functional group.

Two possible amines, secondary and tertiary AAP analogues, were initially screened in the protection assay (Figure 2) and for in vitro microsomal stability (Table 1) and Caco-2 permeability (Table 2). Introduction of the nitrogen led to a potency decrease in the cell-based protection assay; however, the tertiary arylazanyl analogue had a slightly better activity over the secondary arylazanyl analogue. The solubilities of **2** and **3** were good in aqueous media (≥150 μM), and no precipitation occurred at the highest concentration. The in vitro plasma half-life for both compounds was > 60 min. Tertiary amine **3** exhibited a remarkable stability enhancement in human liver microsomes compared with the moderate half-life and clearance rates of the ether and secondary amine analogues. Whereas **1** had excellent permeability and low efflux potential toward Caco-2, neither **2** nor **3** exhibited satisfactory Caco-2 permeability and both had high efflux potential, although **3** was superior to **2**.

These preliminary results suggest that the AAPs may not be an improvement over the aryloxanylpyrazolone series, but the tertiary amine analogue (**3**) showed improved human microsome stability, so a library of tertiary amine analogues was synthesized.

SAR of AAP analogues

Compound activity was determined using the previously described cytotoxicity protection assay (Table 1, Supporting Information).[15] The variability of the EC_{50} values is about a factor of 2. As shown in Figure 1, the tertiary amine AAP scaffold contains four sub-structural moieties: aromatic ring, N-substituent, linker, and the pyrazolone. Structural modifications were conducted on each moiety. A variety of substituents in the aryl moiety was investigated using our previous synthetic method for amination of anilines and γ-halogen-β-ketoesters (Figure 3). In general, the potencies of these AAPs were slightly poorer than the ether counterparts (compound **1** vs **3** [25]). Our previous reports on arylsulfanyl-[16] and aryloxanylpyrazolones[17] (AXP), showed that the 3,5-dichloro substitution pattern in the aromatic ring gave greater potency over the other substitution patterns (about 5-10 fold enhancement). Here, neither the electronic properties (compounds **4-6**) nor the positions of substitution (compounds **9-11**) in the aromatic ring exhibited a large activity change, but the size of the substituents affected the activity in the following order: F < CN < OMe < Cl ~ Br < di-Cl ~ naphthalene. 2,4-Dichloro- and α-naphthyl substitution in the aromatic ring moiety were the most effective.

With the aromatic ring substituents, linker, and pyrazolone held constant, a series of N-substituted AAPs was synthesized (Figure 4; these compounds were being synthesized prior to the measurements in Figure 3, so 3,5-dichloro was selected for aryl substitution). Although the range of potency changed by less than four-fold, the ethyl analogue was the

most potent and the potency decreased with an increase of the size of substituents in the following order: Et > c-Pr > i-Pr ~ Bn > propargyl > t-Bu ~ Ph; however, the smaller methyl analogue was comparable in potency to the cyclopropyl analogue. The propargyl analogue will be beneficial to our ongoing target identification studies, providing a terminal triple bond for reporter group attachment via click chemistry.[26]

An investigation of the linker between the aryl moiety and the pyrazolone also was carried out to determine the influence of length and shape. As shown in Figure 5, one carbon is the optimal length between the nitrogen and the pyrazolone moiety; longer linkers reduce the activity.

One useful modification to enhance the pharmacokinetic properties is a ring-chain transformation.[27] Four ring linkers were introduced to the AAP scaffold (**25-28**). The connection between the aryl group and the N-substituent (**25** and **26**) favored **26**; the linker between the N-substituent and the pyrazolone ring (**27** and **28**) has a preference for that described by **28**. The latter two compounds reveal that substitution at the 5-position of the pyrazolone does not affect potency.

Selected compounds were tested with cortical neurons, which is critical prior to the expensive and time-consuming ALS mouse model studies.[28] Although long linker compound **24** and cyclic linker compound **27** are active in the PC12 assay, they are not active with cortical neurons. Compound **3** gave better results than the ether counterpart (**1**), recovering 100% neuronal activity at 10 μM concentration (Supporting Information).

The pharmacophoric nature of the pyrazolone ring

According to our previous studies, the pyrazolone ring is the key functional group for activity in all of the AXP scaffolds. The compounds without a pyrazolone or with N,N'-dimethyl substituted pyrazolone in aryloxanyl series had no activity.[17] Given that there are three potential H-bonding donors/acceptors in the pyrazolone ring, a determination of their pharmacophoric nature is important. In our recent paper,[18] a putative explanation for the pyrazolone activity was the availability of the N^2-hydrogen (**3a**-type) for hydrogen bonding. To determine if the same moiety was essential for the AAP class of compounds, single N^2-nitrogen substituted pyrazolone analogue **31** and other N2-substituted analogues were synthesized (Scheme 3). As shown in Figure 6, **29** and **30** were comparable in activity to parent compound **3**, while compounds **31-34**, all of which do not have a N^2-H, were devoid of activity, demonstrating the significance of the N^2-H for activity in this series as well.

Several spectrometric analyses were carried out to determine if the pyrazolone structure shown in Figure 6 is most prevalent. Because of a rapid equilibrium among the pyrazolone tautomers, the ^{13}C-NMR spectrum of **3** gave a carbon signal with obscure bumps in the region of the pyrazolone and methylene group. However, clear ^{13}C-NMR spectra of those carbons in **30** and **31** suggested a predominant tautomer. HSQC, HMBC, and NOE spectra of **30** and **31** were then collected. The HSQC spectrum permitted the assignment of all of the protons with their bonding carbons. Analysis of the HMBC spectrum enabled the connectivity of the phenyl, the linker, and the pyrazolone moieties. The cross peaks between the phenol hydrogen and the 4-hydrogen of the pyrazolone in the NOE spectrum determined the spatial approach of these two neighboring hydrogens, which supported the predominant tautomer in **30** and **31** as the phenol form (**30b** and **31b**, Figure 7).

In an attempt to rationalize these observations, comprehensive theoretical calculations were performed on the four possible tautomers of **3** using density-functional theory (DFT); the predicted energy order was d < b < c < a in the gas phase (Table 3). The largest energy difference among all of the forms is 22.6 kJ/mol, which is an insufficient energy barrier to

detect a preferred tautomeric form. Since the tautomerization of pyrazolone was first discovered by Knorr in 1895,[29] several reported calculations have predicted a similar prediction for the stability of the pyrazolone tautomers,[30] and calculations of similar structures predicted that the phenol forms are favored for 1- or 2-substituted pyrazolones in aprotic solvents,[20,31] as we observed.

To further characterize the predominant tautomeric form of the pyrazolone heterocycles in **30** and **31**, we performed quantum chemical calculations (Figure 8). The predominant conformation can be identified by comparing the experimental IR spectra with the predicted IR spectra of the different tautomers. All of the predicted spectra of keto tautomers have a similar high frequency at ~1730 cm^{-1}, while the spectra of phenol-type tautomers have no absorption band in the same region. Hence, the frequency at ~1730 cm^{-1}, the stretching vibration of the C=O bond, is an important band to differentiate these two tautomers. The experimental IR spectra do not contain a band at 1730 cm^{-1}. Furthermore, the most highly predictive bands for phenol forms are in good agreement with the experimental data. All of these results indicate that phenol forms of **30** and **31** are the more stable tautomers. Similar NOE and IR spectral observations for ether analogue **38**[32] suggest that the active pyrazolone tautomer in the AOP series also is the phenol form (see Supporting Information and Figure 8C).

On the basis of the above results, we conclude that the pyrazolone phenol-type tautomer is predominant in solution and in solid phase, but, given that the target(s) is unknown, we cannot conclude definitively whether this tautomer is the pharmacophoric core responsible for the activity of all AAP and AOP analogues. If that tautomer is the active tautomer, then biological activity requires the following two criteria: 1) N^2 has unsubstituted sp^2 hybridization rather than sp^3 hybridization; 2) there is a phenol hydrogen, presumably as a H-bonding donor. The loss of activity by di- and trimethyl substituted derivatives also supports the hypothesis that both criteria must be met for activity.

Conclusion

Aryloxanyl analogues were previously identified as potential drug candidates exhibiting good potency, ADME properties, and equivalent or slightly better results with the ALS mouse model as did the FDA-approved drug riluzole. However, because of its structural limitations, the aryloxanyl analogues may not be suitable as a chemical probe for a biological target study and need further optimization to improve in vivo activity.

The AAP analogues showed superior properties relative to the corresponding ether derivative in potential structural diversity and in preliminary metabolic studies. Conclusions from the SAR study are as follows: (1) the size of the aryl moiety, rather than the electronic properties, is important for good potency; (2) potency decreases when the size of the N-substituents increase; as a potential chemical reporter, the alkynyl group is well tolerated; (3) one carbon is the optimum length for the linker; the linker can be linear or cyclic; (4) the pyrazolone moiety is the only critical pharmacophore of this structure for activity, which prefers the phenol-type tautomer in solution and solid phase, although it is not known if it binds to any targets in that form; (5) a comparison of the predicted and experimental IR spectra is useful to identify the predominant tautomer of a heterocyclic system.

These results support further development of AAP analogues as a reagent for target identification and as a novel drug candidate for the treatment of ALS.

Experimental section

General experimental methods

All reaction were carried out with magnetically stirring and were monitored by thin-layer chromatography on precoated silica gel 60 F254 plates. Column chromatography was performed with silica gel 60 (230 – 400 mesh). Proton and carbon NMR spectra were recorded in deuterated solvents on a Bruker Ag500 (500 MHz) spectrometer. The chemical shifts were reported in δ (ppm) (^{1}H NMR: $CDCl_3$, δ 7.26 ppm; DMSO-d_6, δ 2.50 ppm; ^{13}C NMR: δ 77.23 ppm; DMSO-d_6, δ 39.52 ppm). The following abbreviations were used to define the multiplicities: s = singlet, d = doublet, t = triplet, q = quartet, p = pentet, m = multiplet. Electrospray mass spectra (ESIMS) were obtained using an Agilent 1100 MSD with methanol as the solvent in the positive ion mode. IR was recorded on a Bruker tensor FT-IR spectrometer. Elemental microanalysis was performed by Atlantic Microlab Inc. (Norcross, GA). The C, H, and N analyses were performed by combustion using automatic analyzers, and all of the compounds analyzed showed >95% purity. All reagents purchased from Aldrich, Alfa Aesar, and TCI were used without further purification unless stated otherwise.

General procedure A for nucleophilic amination of anilines and bromoacetates

To a solution of K_2CO_3 (200 mol %) and the aniline (1.0 equiv) in DMF (2 mL/mmol) was added ethyl bromoacetate (150 mol %). The reaction mixture was stirred at room temperature or 80 °C for 16 h. The reaction solution was diluted with ethyl acetate, washed twice with water to remove the reaction solvent, and washed with brine. The collected organic layers were combined, dried over Na_2SO_4, filtered, and concentrated. The crude product was purified on a silica gel column, eluting with a mixture of ethyl acetate and hexane (5% to 20% ethyl acetate) to afford the product as a colorless to pale yellow oil in a yield of 30%-80%.

General procedure B for carbene insertion of anilines

To a solution of the aniline (1.0 equiv) and $Rh_2(OAc)_4$ (2 mol%) in anhydrous dichloromethane (1 mL/mmol) was added ethyl diazoacetate dropwise. Caution: much N_2 is released! The reaction mixture was stirred at room temperature for 1 h. After evaporating the volatiles, the reaction residue was purified on a silica gel column, eluting with a mixture of ethyl acetate and hexane (5% to 20% ethyl acetate) to afford the product as a colorless to pale yellow oil in a yield of 50%-95%.

General procedure C for the synthesis of β-ketoesters from aminoacetates

Ethyl acetate (110 mol%) was added to a THF (5 mL/mmol) solution of LiHMDS (1 N in THF, 120 mol%) at -78 °C and stirred for 60 min. A THF (1 mL/mmol) solution of β-aminoacetate (1.0 equiv) was added dropwise to the reaction mixture at −78 °C. After the resulting solution was stirred at −78 °C for another 2 h, the reaction mixture was quenched with saturated NH_4Cl. The aqueous layer was extracted with ethyl acetate, washed twice with water and brine. The collected organic layers were combined, dried over Na_2SO_4, filtered, and concentrated. The crude product was purified on a silica gel column, eluting with a mixture of ethyl acetate and hexane (10% to 30% ethyl acetate) to afford the product as a colorless to pale yellow oil in a yield of 40%-80%.

General procedure D for direct amination of γ-halo-β-ketoesters with anilines

To a solution of $NaHCO_3$ (200 mol%), NaI (200 mol%), and the aniline (1 equiv) in acetonitrile (1 mL/mol) was added ethyl α-chloracetoacetate (200 mol%). The resulting reaction mixture was stirred at room temperature or at 80 °C for 1-16 h. After the mixture

was cooled to room temperature, saturated $Na_2S_2O_3$ solution (1 mL/mol) was added. The resulting solution was extracted with ethyl acetate, and the organic layer was collected, which was then washed with water and brine. The collected organic layers were combined, dried over Na_2SO_4, filtered, and concentrated. The residue was subjected to column chromatography eluting with a mixture of hexane and ethyl acetate (10% to 30% ethyl acetate) to afford the product as a pale yellow oil in a yield specified in the our published method of amination.[18]

General procedure E for the synthesis of pyrazolones from β-ketoesters

To a solution of β-ketoesters (1 equiv) in EtOH (5 mL/mmol) was added anhydrous hydrazine (200 mol%). The resulting solution was stirred at room temperature overnight. After evaporating the volatiles, the reaction residue was purified on a silica gel column, eluting with a mixture of MeOH and dichloromethane (2% to 10% MeOH) to afford the product as a colorless to pale pink solid. The solid was then recrystallized in dichloromethane/hexane to give the pure product as a white solid in a yield of 60%-75%.

5-((3,5-Dichlorophenylamino)methyl)-1H-pyrazol-3(2H)-one (2)

Following general procedures A, C, and E provided the phenylsulfonyl protected N-(3,5-dichloro phenyl)-N-((5-oxo-2,5-dihydro-1H-pyrazol-3-yl)methyl) benzenesulfonamide. ^{1}H NMR (DMSO-d_6, 500 MHz): δ = 11.56 (br s, 1H), 9.45 (br s, 1H), 7.78-7.74 (m, 1H), 7.64-7.63 (m, 4H), 7.56 (s, 1H), 7.14 (d, J = 1.5 Hz, 2H), 5.21 (s, 1H), 4.67 (s, 2H); ^{13}C NMR (DMSO-d_6, 125 MHz): δ = 140.8, 136.6, 133.8X2, 133.7X2, 129.6X2, 127.6X2, 127.5, 127.0 ppm; MS (ESI): m/z 398.0 $[M+H]^+$.

N-(3,5-dichlorophenyl)-N-((5-oxo-2,5-dihydro-1H-pyrazol-3-yl)methyl) benzenesulfonamide (398 mg, 1 mmol) and 4-hydroxybenzoic acid (800 mg, 5.8 mmol, 200% weight) were added to a solution of HBr (48% in H_2O, 4 mL) and AcOH (4 mL). After the resulting suspension was stirred at 100 °C for 2 h, the reaction mixture was partitioned between 1N HCl (10 mL) and ethyl acetate (30 mL × 2). The collected organic layers were combined, dried over Na_2SO_4, filtered, and concentrated. The residue was subjected to column chromatography eluting with a mixture of MeOH and dichloromethane (5% MeOH) to afford **2** (142 mg, 55% yield) as a white solid. ^{1}H NMR (DMSO-d_6, 500 MHz): δ = 6.65 (t, J = 5.5 Hz, 1H), 6.61 (s, 1H), 6.59, (s, 2H), 5.35 (s, 1H), 4.10 (d, J = 5.0 Hz, 2H); ^{13}C NMR (DMSO-d_6, 125 MHz): δ = 150.7, 134.3X2, 114.6, 110.4X2 ppm; MS (ESI): m/z 280.0 $[M+Na]^+$; CHN calculated for $C_{10}H_9Cl_2N_3O$: C, 46.53; H, 3.51; N, 16.28; found: C, 46.44; H, 3.61; N, 16.36.

5-(((3,5-Dichlorophenyl)(methyl)amino)methyl)-1H-pyrazol-3(2H)-one (3)

The title compound was prepared according to general procedures D and E. ^{1}H NMR (DMSO-d_6, 500 MHz): δ = 9.93 (br s, 1H), 6.72 (m, 3H), 5.24 (s, 1H), 4.40 (s, 2H), 2.96 (s, 3H); ^{13}C NMR (DMSO-d_6, 125 MHz): δ = 150.8, 134.6X2, 114.8, 110.7X2, 88.1, 47.9, 38.6 ppm; MS (ESI): m/z 272.0 $[M+H]^+$; CHN calculated for $C_{11}H_{11}Cl_2N_3O$: C, 48.55; H, 4.07; N, 15.44; found: C, 48.80; H, 4.13; N, 15.35.

5-((Methyl(phenyl)amino)methyl)-1H-pyrazol-3(2H)-one (4)

The title compound was prepared according to general procedures D and E. ^{1}H NMR (DMSO-d_6, 500 MHz): δ = 7.15 (dt, J = 2.0, 7.5 Hz, 2H), 6.76 (d, J = 8.0 Hz, 2H), 6.63 (t, J = 7.5 Hz, 1H), 5.21 (s, 1H), 4.36 (s, 2H), 2.90 (s, 3H); ^{13}C NMR (DMSO-d_6, 125 MHz): δ = 149.0, 128.9X2, 116.3, 112.7, 88.4, 47.7, 38.3 ppm; MS (ESI): m/z 204.0 $[M+H]^+$; CHN calculated for $C_{11}H_{13}N_3O$: C, 65.01; H, 6.45; N, 20.68; found: C, 64.98; H, 6.34; N, 20.68.

5-(((3-Methoxyphenyl)(methyl)amino)methyl)-1H-pyrazol-3(2H)-one (5)

The title compound was prepared according to general procedures D and E. ^{1}H NMR (DMSO-d_6, 500 MHz): δ = 11.47 (br s, 1H), 9.36 (br s, 1H), 7.04 (t, J = 8.0 Hz, 1H), 6.35 (dd, J = 2.0, 7.5 Hz, 1H), 6.26-6.21 (m, 2H), 5.21 (s, 1H), 4.33 (s, 2H), 3.68 (s, 3H), 2.89 (s, 3H); ^{13}C NMR (DMSO-d_6, 125 MHz): δ = 160.2, 150.3, 129.6, 105.7, 101.6, 99.0, 88.8, 54.8, 38.4 ppm; MS (ESI): m/z 234.1 $[M+H]^+$; CHN calculated for $C_{12}H_{15}N_3O_2$: C, 61.79; H, 6.48; N, 18.01; found: C, 61.77; H, 6.47; N, 18.09.

4-(Methyl((5-oxo-2,5-dihydro-1H-pyrazol-3-yl)methyl)amino)benzonitrile (6)

The title compound was prepared according to general procedures D and E. ^{1}H NMR (DMSO-d_6, 500 MHz): δ = 7.53 (d, J = 8.0 Hz, 2H), 6.82 (d, J = 8.0 Hz, 2H), 5.25 (s, 1H), 4.47 (s, 2H), 3.04 (s, 3H); ^{13}C NMR (DMSO-d_6, 125 MHz): δ = 151.6, 133.2X2, 120.4, 112.2X2, 38.4 ppm; MS (ESI): m/z 251.1 $[M+Na]^+$; CHN calculated for $C_{12}H_{12}N_4O$: C, 63.15; H, 5.30; N, 24.55; found: C, 62.87; H, 5.35; N, 24.34.

5-(((4-Fluorophenyl)(methyl)amino)methyl)-1H-pyrazol-3(2H)-one (7)

The title compound was prepared according to general procedures D and E. ^{1}H NMR (DMSO-d_6, 500 MHz): δ = 11.47 (br s, 1H), 9.34 (br s, 1H), 7.00 (t, J = 4.0 Hz, 2H), 6.75 (ddd, J = 2.5, 4.5, 11.0 Hz, 2H), 5.21 (s, 1H), 4.32 (s, 2H), 2.86 (s, 3H); ^{13}C NMR (DMSO-d_6, 125 MHz): δ = 160.3, 155.6, 153.8, 145.9, 141.5, 115.3, 115.1, 114.1, 114.0, 88.2, 48.5, 38.7 ppm; MS (ESI): m/z 222.1 $[M+H]^+$; CHN calculated for $C_{11}H_{12}FN_3O$: C, 59.72; H, 5.47; N, 18.99; found: C, 59.53; H, 5.56; N, 18.96.

5-(((4-Chlorophenyl)(methyl)amino)methyl)-1H-pyrazol-3(2H)-one (8)

The title compound was prepared according to general procedures D and E. ^{1}H NMR (DMSO-d_6, 500 MHz): δ = 7.16 (t, J = 8.5 Hz, 2H), 6.75 (d, J = 8.5 Hz, 2H), 5.20 (s, 1H), 4.36 (s, 2H), 2.90 (s, 3H); ^{13}C NMR (DMSO-d_6, 125 MHz): δ = 147.8, 128.5X2, 119.9, 114.1X2, 88.3, 47.9, 38.5 ppm; MS (ESI): m/z 238.1 $[M+H]^+$; CHN calculated for $C_{11}H_{12}ClN_3O$: C, 55.59; H, 5.09; N, 17.68; found: C, 55.55; H, 5.17; N, 17.58.

5-(((4-Bromophenyl)(methyl)amino)methyl)-1H-pyrazol-3(2H)-one (9)

The title compound was prepared according to general procedures D and E. ^{1}H NMR (DMSO-d_6, 500 MHz): δ = 7.27 (d, J = 7.5 Hz, 2H), 6.70 (d, J = 7.5 Hz, 2H), 5.21 (s, 1H), 4.36 (s, 2H), 2.90 (s, 3H); ^{13}C NMR (DMSO-d_6, 125 MHz): δ = 148.1, 131.3X2, 114.7X2, 107.4, 88.1, 47.9, 38.4 ppm; MS (ESI): m/z 282.0 $[M+H]^+$; CHN calculated for $C_{11}H_{12}BrN_3O$: C, 46.83; H, 4.29; N, 14.89; found: C, 46.93; H, 4.30; N, 14.87.

5-(((3-Bromophenyl)(methyl)amino)methyl)-1H-pyrazol-3(2H)-one (10)

The title compound was prepared according to general procedures D and E. ^{1}H NMR (DMSO-d_6, 500 MHz): δ = 11.50 (br s, 1H), 9.45 (br s, 1H), 7.08 (t, J = 8.0 Hz, 1H), 6.86 (s, 1H), 6.75 (dt, J = 2.5, 8.0 Hz, 2H), 5.22 (s, 1H), 4.37 (s, 2H), 2.92 (s, 3H); ^{13}C NMR (DMSO-d_6, 125 MHz): δ = 150.3, 130.6, 122.6, 118.5, 114.6, 111.5, 38.4 ppm; MS (ESI): m/z 282.0 $[M+H]^+$; CHN calculated for $C_{11}H_{12}BrN_3O$: C, 46.83; H, 4.29; N, 14.89; found: C, 46.92; H, 4.36; N, 14.87.

5-(((3-Bromophenyl)(methyl)amino)methyl)-1H-pyrazol-3(2H)-one (11)

The title compound was prepared according to general procedures D and E. ^{1}H NMR (DMSO-d_6, 500 MHz): δ = 7.58 (dd, J = 1.0, 8.0 Hz, 1H), 7.30 (dt, J = 1.0, 8.0 Hz, 1H), 7.13 (dd, J = 1.0, 8.0 Hz, 1H), 6.97 (dt, J = 1.0, 8.0 Hz, 1H), 5.24 (s, 1H), 4.02 (s, 2H), 2.62 (s, 3H); ^{13}C NMR (DMSO-d_6, 125 MHz): δ = 150.0, 133.5, 128.4, 124.6, 122.6, 119.2, 39.0

ppm; MS (ESI): m/z 282.0 $[M+H]^+$; CHN calculated for $C_{11}H_{12}BrN_3O$: C, 46.83; H, 4.29; N, 14.89; found: C, 46.86; H, 4.31; N, 14.88.

5-((Methyl(naphthalen-2-yl)amino)methyl)-1H-pyrazol-3(2H)-one (12)

The title compound was prepared according to general procedures D and E. ^{1}H NMR (DMSO-d_6, 500 MHz): δ = 7.70 (t, J = 9.0 Hz, 2H), 7.64 (d, J = 8.5 Hz, 1H), 7.34-7.28 (m, 2H), 7.16 (dt, J = 1.0, 8.0 Hz, 1H), 6.97 (d, J = 2.0Hz, 1H), 5.21 (s, 1H), 4.49 (s, 2H), 3.00 (s, 3H); ^{13}C NMR (DMSO-d_6, 125 MHz): δ = 147.0, 134.6, 128.4, 127.2, 126.4, 126.1, 126.0, 121.9, 116.7, 38.5 ppm; MS (ESI): m/z 254.1 $[M+H]^+$; CHN calculated for $C_{15}H_{15}N_3O$: C, 71.13; H, 5.97; N, 16.59; found: C, 70.94; H, 6.02; N, 16.54.

5-((Methyl(naphthalen-1-yl)amino)methyl)-1H-pyrazol-3(2H)-one (13)

The title compound was prepared according to general procedures D and E. ^{1}H NMR (DMSO-d_6, 500 MHz): δ = 8.27 (d, J = 8.0 Hz, 1H), 7.90 (dt, J = 1.5, 7.5 Hz, 1H), 7.59 (d, J = 8.0 Hz, 1H), 7.53-7.49 (m, 2H), 7.41 (t, J = 8.0 Hz, 1H), 7.14 (d, J = 7.0Hz, 1H), 5.31 (s, 1H), 4.08 (s, 2H), 2.73 (s, 3H); ^{13}C NMR (DMSO-d_6, 125 MHz): δ = 149.0, 134.4, 128.5, 128.3, 125.9, 125.8, 125.4, 123.6, 123.1, 115.7, 39.0 ppm; MS (ESI): m/z 254.1 $[M+H]^+$; CHN calculated for $C_{15}H_{15}N_3O$: C, 71.13; H, 5.97; N, 16.59; found: C, 71.29; H, 6.01; N, 16.51.

5-(((3,4-Dichlorophenyl)(methyl)amino)methyl)-1H-pyrazol-3(2H)-one (14)

The title compound was prepared according to general procedures D and E. ^{1}H NMR (DMSO-d_6, 500 MHz): δ = 7.32 (d, J = 9.0 Hz, 1H), 6.91 (d, J = 3.0 Hz, 1H), 6.74 (dd, J = 3.0, 9.0 Hz, 1H), 5.22 (s, 1H), 4.39 (s, 2H), 2.94 (s, 3H); ^{13}C NMR (DMSO-d_6, 125 MHz): δ = 148.8, 131.3, 130.3, 117.3, 113.5, 112.9, 38.5 ppm; MS (ESI): m/z 272.0 $[M+H]^+$; CHN calculated for $C_{11}H_{11}Cl_2N_3O$: C, 48.55; H, 4.07; N, 15.44; found: C, 48.55; H, 4.04; N, 15.46.

5-(((2,4-Dichlorophenyl)(methyl)amino)methyl)-1H-pyrazol-3(2H)-one (15)

The title compound was prepared according to general procedures D and E. ^{1}H NMR (DMSO-d_6, 500 MHz): δ = 7.53 (d, J = 2.0 Hz, 1H), 7.31 (dd, J = 2.0, 8.5 Hz, 1H), 7.09 (d, J = 8.5 Hz, 1H), 5.20 (s, 1H), 4.05 (s, 2H), 2.64 (s, 3H); ^{13}C NMR (DMSO-d_6, 125 MHz): δ = 147.6, 129.7, 128.5, 127.6, 126.7, 123.3, 39.0 ppm; MS (ESI): m/z 272.0 $[M+H]^+$; CHN calculated for $C_{11}H_{11}Cl_2N_3O$: C, 48.55; H, 4.07; N, 15.44; found: C, 48.33; H, 4.18; N, 15.21.

5-(((3,5-Dichlorophenyl)(ethyl)amino)methyl)-1H-pyrazol-3(2H)-one (16)

The title compound was prepared according to general procedures D and E. ^{1}H NMR (DMSO-d_6, 500 MHz): δ = 6.67 (m, 3H), 5.26 (s, 1H), 4.34 (s, 2H), 3.42 (d, J = 7.0 Hz, 2H), 1.06 (t, J = 7.0 Hz, 3H); ^{13}C NMR (DMSO-d_6, 125 MHz): δ = 149.6, 134.6X2, 114.3, 110.2X2, 44.8, 11.8 ppm; MS (ESI): m/z 286.0 $[M+H]^+$; CHN calculated for $C_{12}H_{13}Cl_2N_3O$: C, 50.37; H, 4.58; N, 14.68; found: C, 50.54; H, 4.58; N, 14.68.

5-(((3,5-Dichlorophenyl)(isopropyl)amino)methyl)-1H-pyrazol-3(2H)-one (17)

The title compound was prepared according to general procedures B, C, and E. ^{1}H NMR (DMSO-d_6, 500 MHz): δ = 7.25-7.21 (m, 3H), 5.11 (s, 1H), 4.17 (s, 2H), 1.12 (m, 9H); ^{13}C NMR (DMSO-d_6, 125 MHz): δ = 150.5, 134.5X2, 114.6, 110.9X2, 48.1, 19.5X2 ppm; MS (ESI): m/z 300.1 $[M+H]^+$; CHN calculated for $C_{13}H_{15}Cl_2N_3O$: C, 52.01; H, 5.04; N, 14.00; found: C, 52.10; H, 5.19; N, 13.87.

5-((tert-Butyl(3,5-dichlorophenyl)amino)methyl)-1H-pyrazol-3(2H)-one (18)

The title compound was prepared according to general procedures B, C, and E. ^{1}H NMR (DMSO-d_6, 500 MHz): δ = 6.68-6.67 (m, 3H), 5.22 (s, 1H), 4.25 (s, 2H), 4.17-4.15 (m, 1H), 1.13 (d, J = 7.0 Hz, 6H); ^{13}C NMR (DMSO-d_6, 125 MHz): δ = 151.4, 133.0X2, 127.4, 123.9, 55.7, 17.8X3 ppm; MS (ESI): m/z 314.1 $[M+H]^+$; CHN calculated for $C_{14}H_{17}Cl_2N_3O$: C, 53.52; H, 5.45; N, 13.37; found: C, 53.45; H, 5.45; N, 13.40.

5-((Cyclopropyl(3,5-dichlorophenyl)amino)methyl)-1H-pyrazol-3(2H)-one (19)

The title compound was prepared according to general procedures B, C, and E. ^{1}H NMR (DMSO-d_6, 500 MHz): δ = 9.42 (br s, 1H), 6.86 (s, 2H), 6.74 (s, 1H), 5.10 (s, 1H), 4.37 (s, 2H), 2.43 (s, 1H), 0.83-0.82 (m, 2H), 0.55 (s, 2H); ^{13}C NMR (DMSO-d_6, 125 MHz): δ = 151.3, 134.2X2, 116.1, 112.3X2, 88.4, 46.7, 32.2, 9.1X2 ppm; MS (ESI): m/z 298.0 $[M+H]^+$; CHN calculated for $C_{13}H_{13}Cl_2N_3O$: C, 52.37; H, 4.39; N, 14.09; found: C, 52.33; H, 4.37; N, 14.89.

5-((Benzyl(3,5-dichlorophenyl)amino)methyl)-1H-pyrazol-3(2H)-one (20)

The title compound was prepared according to general procedures B, C, and E. ^{1}H NMR (DMSO-d_6, 500 MHz): δ = 7.34 (t, J = 7.5 Hz, 2H), 7.25 (t, J = 7.5 Hz, 1H), 7.21 (d, J = 7.5 Hz, 2H), 6.70 (s, 1H), 6.68 (s, 2H), 5.32 (s, 1H), 4.66 (s, 2H), 4.52 (s, 2H); ^{13}C NMR (DMSO-d_6, 125 MHz): δ = 150.0, 137.8, 134.4X2, 128.6X2, 127.0, 126.4X2, 115.0, 110.8X2, 53.8 ppm; MS (ESI): m/z 298.0 $[M+H]^+$; CHN calculated for $C_{17}H_{15}Cl_2N_3O$: C, 58.63; H, 4.34; N, 12.07; found: C, 59.01; H, 4.63; N, 11.83.

5-(((3,5-Dichlorophenyl)(phenyl)amino)methyl)-1H-pyrazol-3(2H)-one (21)

The title compound was prepared according to general procedures B, C,[33] and E. ^{1}H NMR (DMSO-d_6, 500 MHz): δ = 11.59 (br s, 1H), 9.65 (br s, 1H), 7.43 (t, J = 7.0 Hz, 2H), 7.28-7.22 (m, 3H), 6.88 (s, 1H), 6.72 (s, 2H), 5.24 (s, 1H), 4.77 (s, 2H); ^{13}C NMR (DMSO-d_6, 125 MHz): δ = 150.0, 145.6, 134.4X2, 130.0X2, 125.8X2, 125.6, 117.2, 113.8X2 ppm; MS (ESI): m/z 334.0 $[M+H]^+$; CHN calculated for $C_{16}H_{13}Cl_2N_3O$: C, 57.50; H, 3.92; N, 12.57; found: C, 57.70; H, 4.27; N, 12.94.

5-(((3,5-Dichlorophenyl)(prop-2-ynyl)amino)methyl)-1H-pyrazol-3(2H)-one (22)

The title compound was prepared according to general procedures B, C, and E. ^{1}H NMR (DMSO-d_6, 500 MHz): δ = 6.82 (s, 3H), 5.35 (s, 1H), 4.41 (s, 2H), 4.21 (d, J = 2.0 Hz, 2H), 3.26 (d, J = 2.0 Hz, 1H); ^{13}C NMR (DMSO-d_6, 125 MHz): δ = 149.4, 134.4X2, 116.1, 111.8X2, 89.1, 79.6, 75.2 ppm; MS (ESI): m/z 296.1 $[M+H]^+$; CHN calculated for $C_{13}H_{11}Cl_2N_3O$: C, 52.72; H, 3.74; N, 14.19; found: C, 52.63; H, 3.91; N, 13.92.

5-(2-((3,5-Dichlorophenyl)(methyl)amino)ethyl)-1H-pyrazol-3(2H)-one (23)

The title compound was prepared according to general procedures A, C, and E. ^{1}H NMR (DMSO-d_6, 500 MHz): δ = 11.35 (br s, 1H), 9.41 (br s, 1H), 6.69 (d, J = 1.5 Hz, 1H), 6.66 (d, J = 2.0 Hz, 2H), 5.33 (s, 1H), 3.54 (t, J = 7.5 Hz, 2H), 2.85 (s, 3H), 2.64 (t, J = 7.5 Hz, 2H); ^{13}C NMR (DMSO-d_6, 125 MHz): δ = 150.4, 134.7X2, 114.3, 110.0X2, 88.7, 51.1, 37.9 ppm; MS (ESI): m/z 286.0 $[M+H]^+$; CHN calculated for $C_{12}H_{13}Cl_2N_3O$: C, 50.37; H, 4.58; N, 14.68; found: C, 50.66; H, 4.80; N, 14.58.

5-(3-((3,5-Dichlorophenyl)(methyl)amino)propyl)-1H-pyrazol-3(2H)-one (24)

The title compound was prepared according to general procedures B, C, and E. ^{1}H NMR (DMSO-d_6, 500 MHz): δ = 11.27 (br s, 1H), 9.30 (br s, 1H), 6.66 (d, J = 1.5 Hz, 1H), 6.61 (d, J = 1.5 Hz, 2H), 5.26 (s, 1H), 3.32 (t, J = 7.5 Hz, 2H), 2.88 (s, 3H), 2.45 (t, J = 7.5 Hz,

2H), 1.76-1.73 (m, 2H); ^{13}C NMR (DMSO-d_6, 125 MHz): δ = 150.7, 134.7X2, 114.0, 109.8X2, 50.9, 38.0, 25.4 ppm; MS (ESI): m/z 300.1 $[M+H]^+$; CHN calculated for $C_{13}H_{15}Cl_2N_3O$: C, 52.01; H, 5.04; N, 14.00; found: C, 52.23; H, 5.14; N, 14.94.

5-(Indolin-1-ylmethyl)-1H-pyrazol-3(2H)-one (25)

The title compound was prepared according to general procedures D and E. ^{1}H NMR (DMSO-d_6, 500 MHz): δ = 7.02 (d, J = 7.0 Hz, 1H), 6.98 (t, J = 7.5 Hz, 1H), 6.62 (d, J = 7.5 Hz, 1H), 6.58 (t, J = 7.5 Hz, 1H), 5.31 (s, 1H), 4.12 (s, 2H), 3.24 (t, J = 8.0 Hz, 2H), 2.85 (t, J = 8.0 Hz, 2H); ^{13}C NMR (DMSO-d_6, 125 MHz): δ = 151.7, 129.8, 127.0, 124.3, 117.5, 107.5, 89.0, 52.6, 44.0, 27.9 ppm; MS (ESI): m/z 216.1 $[M+H]^+$; CHN calculated for $C_{12}H_{13}N_3O$: C, 66.96; H, 6.09; N, 19.52; found: C, 66.85; H, 6.11; N, 19.44.

5-((3,4-Dihydroquinolin-1(2H)-yl)methyl)-1H-pyrazol-3(2H)-one (26)

The title compound was prepared according to general procedures D and E. ^{1}H NMR (DMSO-d_6, 500 MHz): δ = 6.91 (t, J = 7.0 Hz, 1H), 6.86 (d, J = 7.0 Hz, 1H), 6.64 (d, J = 8.5 Hz, 1H), 6.47 (t, J = 7.5 Hz, 1H), 5.26 (s, 1H), 4.28 (s, 2H), 3.28 (t, J = 5.5 Hz, 2H), 2.66 (t, J = 5.5 Hz, 2H), 1.87 (p, J = 6.0 Hz, 2H); ^{13}C NMR (DMSO-d_6, 125 MHz): δ = 144.9, 128.8, 126.7, 122.2, 115.8, 111.2, 88.4, 49.1, 46.5, 39.0, 27.5, 21.8 ppm; MS (ESI): m/z 216.1 $[M+H]^+$; CHN calculated for $C_{13}H_{15}N_3O$: C, 68.10; H, 6.59; N, 18.33; found: C, 68.02; H, 6.60; N, 18.29.

5-(3,5-Dichlorophenyl)-4,5,6,7-tetrahydro-1H-pyrazolo[4,3-c]pyridin-3(2H)-one (27)

The title compound was prepared according to the literature procedure[34] and general procedure E. ^{1}H NMR (DMSO-d_6, 500 MHz): δ = 6.95 (s, 2H), 6.82 (d, J = 1.5 Hz, 1H), 4.06 (s, 2H), 3.59 (t, J = 6.0 Hz, 1H), 2.63-2.62 (m, 2H); ^{13}C NMR (DMSO-d_6, 125 MHz): δ = 152.1, 134.7X2, 116.4,112.9X2, 45.0, 43.0 ppm; MS (ESI): m/z 284.0 $[M+H]^+$; CHN calculated for $C_{12}H_{11}Cl_2N_3O$: C, 50.72; H, 3.90; N, 14.79; found: C, 50.53; H, 4.03; N, 14.83.

6-(3,5-Dichlorophenyl)-4,5,6,7-tetrahydro-1H-pyrazolo[3,4-c]pyridin-3(2H)-one (28)

The title compound was prepared according to the literature procedure[27] and general procedure E. ^{1}H NMR (DMSO-d_6, 500 MHz): δ = 6.96 (d, J = 1.5 Hz, 2H), 6.83 (d, J = 1.5 Hz, 1H), 4.26 (s, 2H), 3.55 (t, J = 6.0 Hz, 2H), 3.16 (d, J = 5.0 Hz, 1H), 2.41-2.39 (m, 2H); ^{13}C NMR (DMSO-d_6, 125 MHz): δ = 152.0, 134.7X2, 116.6, 113.1X2, 46.2, 29.5, 18.6 ppm; MS (ESI): m/z 284.0 $[M+H]^+$; CHN calculated for $C_{12}H_{11}Cl_2N_3O$: C, 50.72; H, 3.90; N, 14.79; found: C, 50.51; H, 3.78; N, 14.57.

2-Benzyl-5-(((3,5-dichlorophenyl)(methyl)amino)methyl)-1H-pyrazol-3(2H)-one (29)

To a solution of ethyl 4-((3,5-dichlorophenyl)(methyl)amino)-3-oxobutanoate (304 mg, 1.0 mmol) and benzyl hydrazine chloride (388 mg, 2.0 mmol) in EtOH (5 mL) was added anhydrous triethylamine (570 uL, 4.0 mmol). The resulting solution was stirred at room temperature overnight. After evaporating the volatiles, the residue was purified on a silica gel column, eluting with a mixture of MeOH and dichloromethane (1% to 2% MeOH) to afford the product as a pale yellow solid (320 mg, 88%). The solid was then recrystallized in dichloromethane/hexane to give the product as a white solid. ^{1}H NMR (DMSO-d_6, 500 MHz): δ = 11.00 (br s, 1H), 7.28 (t, J = 7.0 Hz, 2H), 7.23 (d, J = 7.0 Hz, 1H), 7.11 (d, J = 7.0 Hz, 2H), 6.74 (d, J = 1.5 Hz, 2H), 6.69 (s, 1H), 5.12 (s, 1H), 5.01 (s, 2H), 4.33 (s, 2H), 2.98 (s, 2H); ^{13}C NMR (DMSO-d_6, 125 MHz): δ = 152.7, 151.0, 146.8, 138.0, 134.4X2, 128.4X2, 127.1, 127.0X2, 114.4, 110.6X2, 84.6, 50.3, 49.2, 38.9 ppm; MS (ESI): m/z 284.0 $[M+H]^+$; CHN calculated for $C_{18}H_{17}Cl_2N_3O$: C, 59.68; H, 4.73; N, 11.60; found: C, 59.79; H, 4.68; N, 11.48.

5-(((3,5-Dichlorophenyl)(methyl)amino)methyl)-2-methyl-1H-pyrazol-3(2H)-one (30)

To a solution of ethyl 4-((3,5-dichlorophenyl)(methyl)amino)-3-oxobutanoate (304 mg, 1.0 mmol) in EtOH (5 mL) was added anhydrous methyl hydrazine (105 uL, 2.0 mmol). The resulting solution was stirred at room temperature overnight. After evaporating the volatiles, the residue was purified on a silica gel column, eluting with a mixture of MeOH and dichloromethane (2% to 10% MeOH) to afford the product as a pale yellow solid (231 mg, 81%). The solid was then recrystallized in dichloromethane/hexane to give the product as a white solid. ^{1}H NMR (DMSO-d_6, 500 MHz): δ = 6.72 (d, J = 1.5 Hz, 2H), 6.68 (t, J = 1.5 Hz, 1H), 5.13 (s, 1H), 4.29 (s, 2H), 3.43 (s, 3H), 2.95 (s, 3H); ^{13}C NMR (DMSO-d_6, 125 MHz): δ = 152.5, 151.0, 146.0, 134.4X2, 114.3, 110.4X2, 84.5, 49.9, 38.5, 33.0 ppm; MS (ESI): m/z 286.1 $[M+H]^+$; CHN calculated for $C_{12}H_{13}Cl_2N_3O$: C, 50.37; H, 4.58; N, 14.68; found: C, 50.60; H, 4.65; N, 14.62; FTIR (solid), ν 1591, 1552, 1495, 1445, 1309, 1272, 1094, 1012, 980, 950, 813, 756, 662 cm^{-1}; (DMSO), ν 1591, 1552, 1436, 1309, 1042 (bw), 950, 806, 756, 697, 663 cm^{-1}.

5-(((3,5-Dichlorophenyl)(methyl)amino)methyl)-1-methyl-1H-pyrazol-3(2H)-one (31)

Compound **37** (115 mg, 0.37 mmol) was suspended in 2 N HCl (7 mL) and stirred at 60 °C overnight. Ethyl acetate was added to the mixture, and the organic layer was separated, washed with water and brine, dried over Na_2SO_4, and concentrated. The residue was purified on a silica gel column, eluting with a mixture of MeOH and dichloromethane (4% MeOH) to afford the product as a white solid (55 mg, 52%). ^{1}H NMR (DMSO-d_6, 500 MHz): δ = 9.42 (s, 1H), 6.75 (m, 3H), 5.08 (s, 1H), 4.54 (s, 2H), 3.52 (s, 3H), 2.94 (s, 3H); ^{13}C NMR (DMSO-d_6, 125 MHz): δ = 159.5, 150.8, 139.4, 134.6X2, 115.0, 110.7X2, 89.7, 46.9, 38.2, 35.7 ppm; MS (ESI): m/z 286.1 $[M+H]^+$; CHN calculated for $C_{12}H_{13}Cl_2N_3O$: C, 50.37; H, 4.58; N, 14.68; found: C, 50.57; H, 4.73; N, 14.74; FTIR (solid), ν 1587, 1552, 1493, 1447, 1345, 1125, 1098, 1018, 959, 813, 801, 774, 663 cm^{-1}; (DMSO), ν 1587, 1552, 1493, 1435, 1282, 1043 (bw), 952, 800, 697, 664 cm^{-1}.

5-(((3,5-Dichlorophenyl)(methyl)amino)methyl)-1,2,4-trimethyl-1H-pyrazol-3(2H)-one (32)

The solution of compound **30** (200 mg, 0.7 mmol), MeI (132 uL, 2.1 mmol), and K_2CO_3 (290 mg, 2.1 mmol) in acetonitrile (3.5 mL) was stirred at 50 °C for 24 h. After evaporating the volatiles, the residue was purified on a silica gel column, eluting with a mixture of MeOH and dichloromethane (1%-5% MeOH) to afford the product (compounds **32**-**34**) as a pale yellow solid or liquid.

^{1}H NMR ($CDCl_3$, 500 MHz): δ = 6.78 (t, J = 1.5 Hz, 1H), 6.65 (d, J = 1.5 Hz, 2H), 4.23 (s, 2H), 3.32 (s, 3H), 3.08 (s, 3H), 2.82 (s, 3H), 1.86 (s, 3H); ^{13}C NMR ($CDCl_3$, 125 MHz): δ = 166.5, 151.1, 147.3, 136.0X2, 118.2, 111.9X2, 108.7, 46.7, 37.6, 35.0, 29.1, 7.27 ppm; MS (ESI): m/z 314.1 $[M+H]^+$.

5-(((3,5-Dichlorophenyl)(methyl)amino)methyl)-1,2-dimethyl-1H-pyrazol-3(2H)-one (33)

^{1}H NMR ($CDCl_3$, 500 MHz): δ = 6.76 (t, J = 1.5 Hz, 1H), 6.57 (d, J = 2.0 Hz, 2H), 5.28 (s, 1H), 4.27 (s, 2H), 3.38 (s, 3H), 3.25 (s, 3H), 2.96 (s, 3H); ^{13}C NMR ($CDCl_3$, 125 MHz): δ = 166.0, 151.4, 150.4, 135.9X2, 118.0, 111.4X2, 98.1, 49.0, 38.7, 34.2, 28.8 ppm; MS (ESI): m/z 300.1 $[M+H]^+$.

3-(((3,5-Dichlorophenyl)(methyl)amino)methyl)-1,4,4-trimethyl-1H-pyrazol-5(4H)-one (34)

^{1}H NMR ($CDCl_3$, 500 MHz): δ = 6.72 (t, J = 1.5 Hz, 1H), 6.58 (d, J = 1.5 Hz, 2H), 4.17 (s, 2H), 3.30 (s, 3H), 3.00 (s, 3H), 1.23 (s, 6H); ^{13}C NMR ($CDCl_3$, 125 MHz): δ = 178.4, 162.6, 150.6, 135.8X2, 117.2, 110.9X2, 50.6, 48.0, 39.3, 31.5, 21.3 ppm; MS (ESI): m/z 314.1 $[M+H]^+$.

3,5-Dichloro-N-((2,3-dihydropyrazolo[5,1-b]oxazol-6-yl)methyl)-N-methylaniline (36)

To a solution of ethyl 4-((3,5-dichlorophenyl)(methyl)amino)-3-oxobutanoate (304 mg, 1.0 mmol) in EtOH (5 mL), 2-hydroxyethylhydrazine (85 uL, 1.1 mmol) was added and stirred for 3 h. After evaporating the volatiles, the residues were dissolved with dry acetonitrile (10 mL) and triethylamine (156 uL, 1.1 mmol) followed by the addition of tosyl chloride (190 mg, 1.0 mmol). The solution was stirred for 20 min, diluted in ethyl acetate (20 mL), washed with water (10 mL), dried over Na_2SO_4, and concentrated. The residue was purified on a silica gel column, eluting with a mixture of MeOH and dichloromethane (2% MeOH) to afford the product as a pale yellow liquid **35** (400 mg, 85%).

Under an inert atmosphere, **35** was dissolved in anhydride acetonitrile (8.5 mL) followed by the addition of sodium hydride (40 mg, 1.0 mmol). The mixture was stirred overnight at room temperature and evaporated to give the residue, which was purified on a silica gel column, eluting with a mixture of MeOH and dichloromethane (1% MeOH) to afford the product as a pale yellow solid **36** (200 mg, 79%). ^{1}H NMR ($CDCl_3$, 500 MHz): δ = 6.66 (d, J = 1.5 Hz, 1H), 6.63 (d, J = 1.5 Hz, 2H), 5.19 (s, 1H), 5.00 (dd, J = 7.5, 9.0 Hz, 2H), 4.36 (s, 2H), 4.25 (t, J = 7.5 Hz, 2H), 2.99 (s, 3H); ^{13}C NMR ($CDCl_3$, 125 MHz): δ = 159.7, 155.0, 151.0, 135.6X2, 116.4, 111.0X2, 79.5, 75.3, 51.6, 45.4, 38.8 ppm; MS (ESI): m/z 298.0 $[M+H]^+$.

5-(((3,5-Dichlorophenyl)(methyl)amino)methyl)-1-methyl-2-vinyl-1H-pyrazol-3(2H)-one (37)

To a solution of compound **36** (200 mg, 0.67 mmol) in anhydrous acetonitrile (6 mL), methyl trifluoromethanesulfonate (85 uL, 0.75 mmol) was added, and the solution was stirred for 2 h before the addition of sodium iodide (195 mg, 1.3 mmol) and TsOH (127 mg, 0.67 mmol). After conversion to the iodinated intermediate by overnight stirring, KOtBu (188 mg, 1.7 mmol) was added to the mixture, which was further stirred for 1 h. After evaporating the volatiles, the residue was purified on a silica gel column, eluting with a mixture of MeOH and dichloromethane (4% MeOH) to afford the product as a yellow liquid (115 mg, 55%). ^{1}H NMR ($CDCl_3$, 500 MHz): δ = 6.85 (dd, J = 9.0, 16.0 Hz, 1H), 6.77 (t, J = 1.5 Hz, 2H), 6.56 (d, J = 1.5 Hz, 2H), 5.37 (s, 1H), 4.88-4.80 (m, 2H), 4.31 (s, 2H), 3.17 (s, 3H), 2.99 (s, 3H); ^{13}C NMR ($CDCl_3$, 125 MHz): δ = 165.4, 159.2, 150.3, 136.0X2, 126.3, 118.0, 111.3X2, 101.1, 99.5, 49.6, 39.0, 37.3 ppm.

Mutant SOD1-induced cytotoxicity protection assay

Viability and EC_{50} values were determined for **1a, 1b, 2a**, and **2b** according to the previously reported assay procedure.[15] PC12 cells were seeded at 15000 cells/well in 96-well plates and incubated 24 h prior to compound addition. Compounds were assayed in 12-point dose-response experiments to determine potency and efficacy. The highest compound concentration tested was 32 μM, which was decreased by one-half with each subsequent dose. After a 24 h incubation with the compounds, MG132 was added at a final concentration of 100 nM. MG132 is a well-characterized proteasome inhibitor, which would be expected to enhance the appearance of protein aggregation by blocking the proteosomal clearance of aggregated proteins. Cell viability was measured 48 h later using the fluorescent viability probe, Calcein-AM (Molecular Probes). Briefly, cells were washed twice with PBS, Calcein-AM was added at a final concentration of 1 μM for 20 min at room temperature, and fluorescence intensity was read in a POLARstar fluorescence plate reader (BMG). Fluorescence data were coupled with compound structural data, then stored, and analyzed using the CambridgeSoft Chemoffice Enterprise Ultra software package.

In vitro ADME assays

In vitro microsomal stability, aqueous solubility, and Caco-2 permeability were determined for **1b** and **2b** at Apredica Inc. (Watertown, MA).

Computational Methods

Possible initial tautomer structures were constructed with molecular modeling software Sybyl-X 1.2 (Tripos International, St. Louis, MO). After primary optimization by use of MM2 molecular mechanical module encoded in the program CS Chem3D, these two structures were subjected to full optimization within the density-functional theory (DFT). The Lee–Yang–Parr correlation functional approximation (B3LYP) method was used in a 6-31+G(d,p) basis set.[35,36] On the basis of the optimized geometries, energy or frequency calculations were carried out at the same levels of B3LYP so as to verify the reasonability of the optimized structures. A frequency scaling factor of 0.964 was used in the comparison of the calculated results with the experimental spectra.[37] All of the Quantum Chemical calculations were carried out with the Gamess (2012R1) program.[38]

Supplementary Material

Refer to Web version on PubMed Central for supplementary material.

Acknowledgments

We thank the National Institutes of Health (grant 1R43NS057849), the ALS Association (TREAT program), and the Department of Defense (AL093052), for their generous support of this research.

References

1. Rowland LP, Shneider NA. Amyotrophic lateral sclerosis. N Engl J Med. 2001; 344:1688–1700. [PubMed: 11386269]
2. Rothstein JD. Currenthypothese for the underlying biology of amyotrophic lateral sclerosis. Ann Neurol. 2009; 65(Suppl. 1):S3–S9. [PubMed: 19191304]
3. Worms PM. The epidemiology of motor neuron diseases: a review of recent studies. J Neurol Sci. 2001; 191:3–9. [PubMed: 11676986]
4. Weisskopf MG, O'Reilly EJ, McCullough ML, Calle EE, Thun MJ, Cudkowicz M, Ascherio A. Prospective study of military service and mortality from ALS. Neurology. 2005; 64:32–37. [PubMed: 15642900]
5. Mitsumoto H, Rabkin JG. Palliative care for patients with amyotrophic lateral sclerosis: "Prepare for the worst and hope for the best". J Am Med Assoc. 2007; 298:207–216.
6. Waldmeier PC, Tatton WG. Interrupting apoptosis in neurodegenerative disease: potential for effective therapy? Drug Discov Today. 2004; 9:210–218. [PubMed: 14980539]
7. Bensimon G, Lacomblez L, Meininger VA. controlled trial of riluzole in amyotrophic lateral sclerosis. ALS/Riluzole Study Group. N. Engl J Med. 1994; 330:585–591.
8. See http://alsod.iop.kcl.ac.uk/ The ALS online genetics database
9. Rosen DR, Siddique T, Patterson D, Figlewicz DA, Sapp P, et al. Mutations in Cu/Zn superoxide dismutase gene are associated with familial amyotrophic lateral sclerosis. Nature. 1993; 362:59–62. [PubMed: 8446170]
10. Turner BJ, Talbot K. Transgenics, toxicity and therapeutics in rodent models of mutant SOD1-mediated familial ALS. Prog Neurobiol. 2008; 85:94–134. [PubMed: 18282652]
11. Nagai M, Re DB, Nagata T, Chalazonitis A, Jessell TM, Wichterle H, Przedborski S. Astrocytes expressing ALS-linked mutated SOD1 release factors selectively toxic to motor neurons. Nat Neurosci. 2007; 10:615–622. [PubMed: 17435755]
12. Haidet-Phillips AM, Hester ME, Miranda CJ, Meyer K, Braun Ashley Frakes L, Song SW, Likhite S, Murtha MJ, Foust KD, Rao M, Eagle A, Kammesheidt A, Christensen A, Mendell JR, Burghes

AHM, Kaspar BK. Astrocytes from familial and sporadic ALS patients are toxic to motor neurons. Nature Biotech. 2011; 29:824–830.

13. Gruzman A, Wood WL, Alpert E, Prasad MD, Miller RG, Rothstein JD, Bowser R, Hamilton R, Wood TD, Cleveland DW, Lingappa VR, Liu J. Common molecular signature in SOD1 for both sporadic and familial amyotrophic lateral sclerosis. Proc Natl Acad Sci USA. 2007; 104:12524–12529. [PubMed: 17636119]
14. Matsumoto G, Stojanovic A, Holmber CI, Kim S, Morimoto RI. Structure properties and neuronal toxicity of amyotrophic lateral sclerosis-associated Cu/Zn superoxide dismutase 1 aggregates. J Cell Biol. 2005; 171:75–85. [PubMed: 16216923]
15. Benmohamed R, Arvanites AC, Silverman RB, Morimoto RI, Ferrante RJ, Kirsch DR. Identification of compounds protective against G93A SOD1 toxicity for the treatment of amyotrophic lateral sclerosis. Amyotrophic Lateral Scler Other Mot Neuron Disord. 2011; 12:87–96.
16. Chen T, Benmohamed R, Arvanites AC, Ranaivo HR, Morimoto RI, Ferrante RJ, Watterson DM, Kirsch DR, Silverman RB. Arylsulfanyl pyrazolones block mutant SOD1-G93A aggregation. Potential application for the treatment of amyotrophic lateral sclerosis. Bioorg Med Chem. 2011; 19:613–622. [PubMed: 21095130]
17. Chen T, Benmohamed R, Kim J, Smith K, Amante D, Morimoto RI, Ferrante RJ, Kirsch D, Silverman RB. ADME-guided design and synthesis of aryloxanylpyrazonlone derivatives to block mutant superoxide dismutase 1 (SOD1) cytotoxicity and protective aggregation: Potential application for the treatment of amyotrophic lateral sclerosis. J Med Chem. 2012; 55:515–527. [PubMed: 22191331]
18. Trippier PC, Benmohammed R, Kirsch DR, Silverman RB. Substituted pyrazolones require N^2 hydrogen bond donating ability to protect against cytotoxicity from protein aggregation of mutant superoxide dismutase 1. Bioorg Med Chem Lett. 2012; 22:6647–6650. [PubMed: 23021992]
19. Zhang Y, Silverman R. Direct amination of γ-halo-β-ketoesters with anilines. J Org Chem. 2012; 77:3462–3467. [PubMed: 22390154]
20. Yang M, Wang X, Li H, Livant P. A new route to hindered tertiary amines. J Org Chem. 2001; 66:6729–6733. [PubMed: 11578227]
21. Hamper BC, Kurtzweil ML, Beck JP. Cyclocodensation of alkyl hydrazines and β-substituted acetylenic esters: synthesis of 3-hydroxypyrazoles. J Org Chem. 1992; 57:5680–5686.
22. Zimmermann D, Krogsgaard-Larsen P, Ehrhard J-D, Madsen U, Janin YL. Unambiguous synthesis of 1-methyl-3-hydroxypyrazoles. Tetrahedron. 1998; 54:9393–9400.
23. Kerns, EH.; Di, L. Drug-like Properties: Concepts, Structure, Design, and Methods. Academic Press; Amsterdam: 2008. p. 65
24. Van de Waterbeemd H, Gifford E. ADMET *in silico* modeling: towards prediction paradise? Nat Rev Drug Dicov. 2003; 2:192–204.
25. Compound **1**, which had an EC_{50} of 0.067 μM in the protection assay in our earlier report of aryloxanyl pyrazolones, showed an average activity of 0.4 μM for several parallel repeats in this study.
26. Park KD, Kim D, Reamtong O, Eyers C, Gaskell SJ, Liu R, Kohn H. Identification of a Lacosamide binding protein using an affinity bait and chemical reporter strategy: 14-3-3ζ. J Am Chem Soc. 2011; 133:11320–11330. [PubMed: 21692503]
27. Silverman, RB. The Organic Chemistry of Drug Design and Drug Action. 2. Elsevier Academic Press; Amsterdam: 2004. p. 28
28. Zhang Y, Benmohamed R, Zhang W, Kim J, Edgerly CK, Zhu Y, Morimoto RI, Ferrante RJ, Kirsch DR, Silverman RB. Chiral cyclohexane 1,3-diones as inhibitors of mutant SOD1-dependent protein aggregation for the treatment of amyotrophic lateral sclerosis. ACS Med Chem Lett. 2012; 3:584–587. [PubMed: 22837812]
29. Knorr L. Ueber abkommlinge der phenol form des 1-phenyl-3-methyl-5-pyrazolons. Ber Dtsch Chem Ges. 1895; 28:706–714.
30. a) Parchment OG, Green DVS, Taylor PJ, Hillier IH. The prediction of tautomer equilibria in hydrated 3-hydroxypyrazole: A challenge to theory. J Am Chem Soc. 1993; 115:2352–2356.b) Enchev V, Neykov GD. A semiempirical and Ab Initios MO study of the tautomers of N-

unsubstituted pyrazolones (hyroxy pyrazoles). Struc Chem. 1992:231–238.c) Nagy PI, Tejada FR, Messer WS Jr. Theoretical studies of the tautomeric equilibria for five-member N-heterocycles in the gas phase and in solution. J Phys Chem B. 2005; 109:22588–22602. [PubMed: 16853941]

31. Hamper B. Regioselective synthesis of 1-methyl-3-hydroxy-5-perfluoroalkyl pyrazoles by the addition of methylhydrazine to perfluoroalkylacetylenic ester. J Fluo Chem. 1990; 48:123–131.
32. Compound **5b** in reference 17.
33. In procedure C for preparing compound **21**, the reaction time needs to be extended to 16 h while allowing the reaction temperature to rise to room temperature.
34. Zhang Y, Silverman RB. An efficient synthesis of 1-aryl-3-piperidione derivative through MBH and RCM reactions. Tetrahedral Lett. 2013; 54:573–575.
35. Becke AD. Density-functional thermochemistry. III. The role of exact exchange. J Chem Phys. 1993; 98:5648–5652.
36. Lee C, Yang W, Parr RG. Development of the Colle-Salvetti conelation energy formula into a functional of the electron density. Phys Rev B. 1988; 37:785–789.
37. Merrick JP, Moran D, Radom L. An Evaluation of Harmonic Vibrational Frequency Scale Factors. J Phys Chem A. 2007; 111:11683–11700. [PubMed: 17948971]
38. Schmidt MS, Baldridge KK, Boatz JA, Elbert ST, Gordon MS, Jensen JH, Koseki S, Matsunaga N, Nguyen KA, Su S, Windus TL, Dupuis M, Montgomery JA. General atomic and molecular electronic structure system. J Comput Chem. 1993; 14:1347–1363.

Abbreviations

AAP	arylazanyl pyrazolone
ADME	absorption, distribution, metabolism, excretion
ALS	amyotrophic lateral sclerosis
ASP	arylsulfanyl pyrazolone
AXP	aryl heteroatom pyrazolone
CNS	central nervous system
DFT	density functional theory
FALS	familial ALS
IR	infrared spectroscopy
NOE	nuclear overhauser effect spectroscopy
PBS	phosphate buffered saline
PK	pharmacokinetics
SALS	sporadic ALS
SOD1	Cu/Zn superoxide dismutase

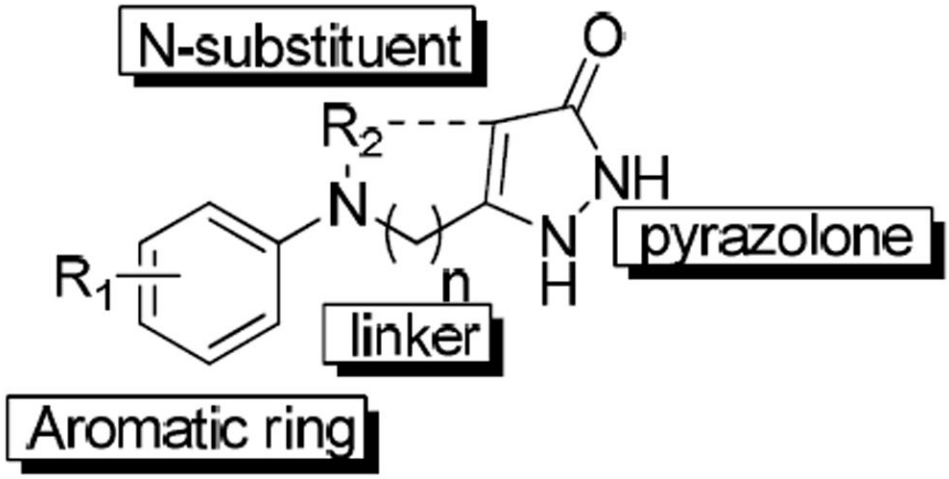

Figure 1.
Sub-structures of AAP analogues

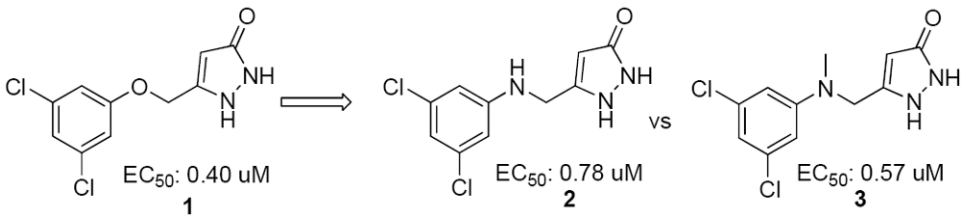

Figure 2.
Conversion of ether linker to amine linker

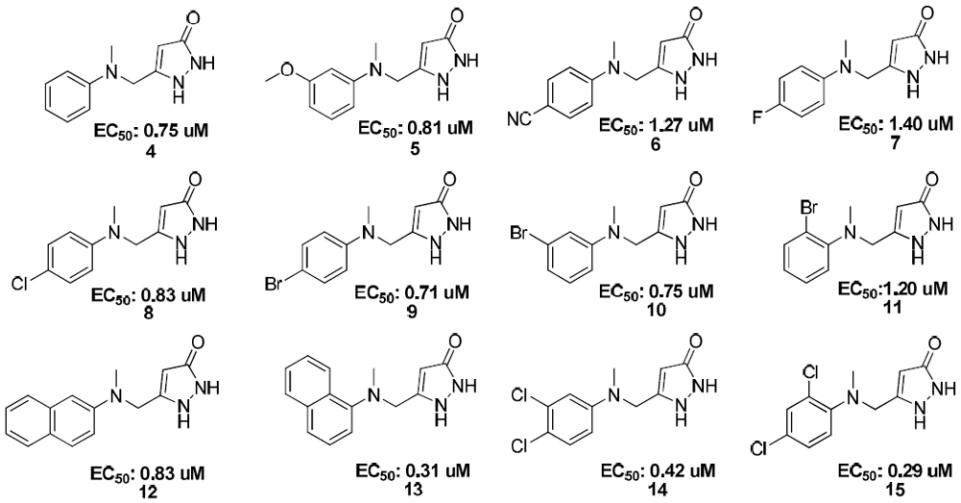

Figure 3.
AAP analogues with different substituents in the aromatic moiety

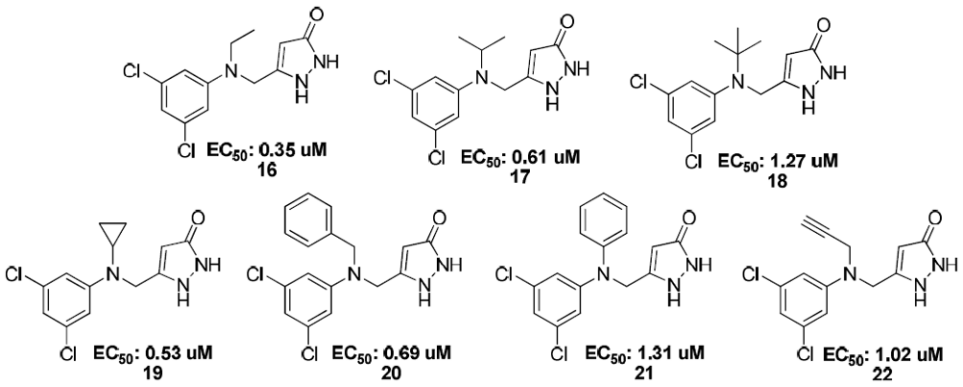

Figure 4.
AAP analogues with different N-substituents

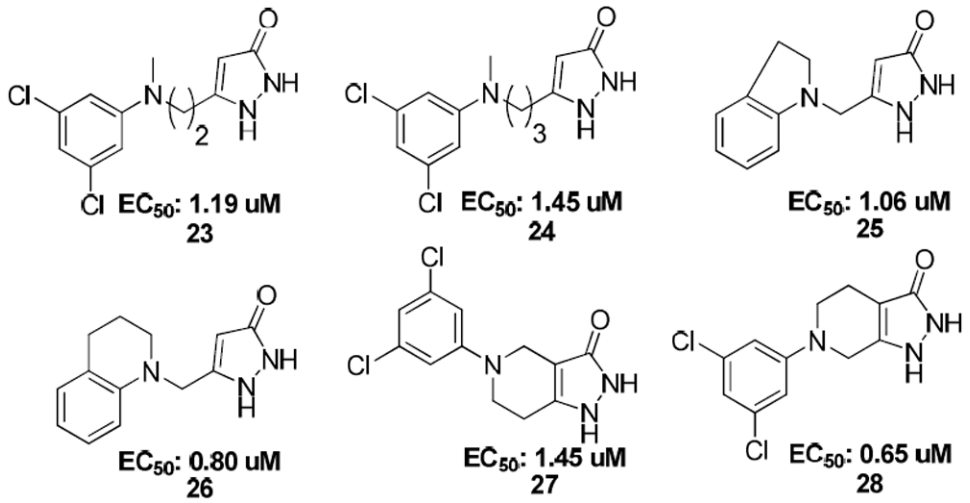

Figure 5.
AAP analogues with different linkers

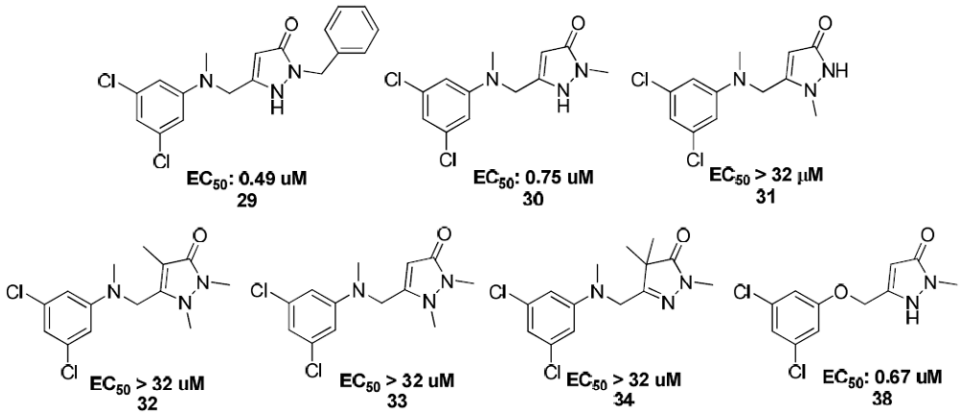

Figure 6.
AAP analogues with different pyrazolone substitutions

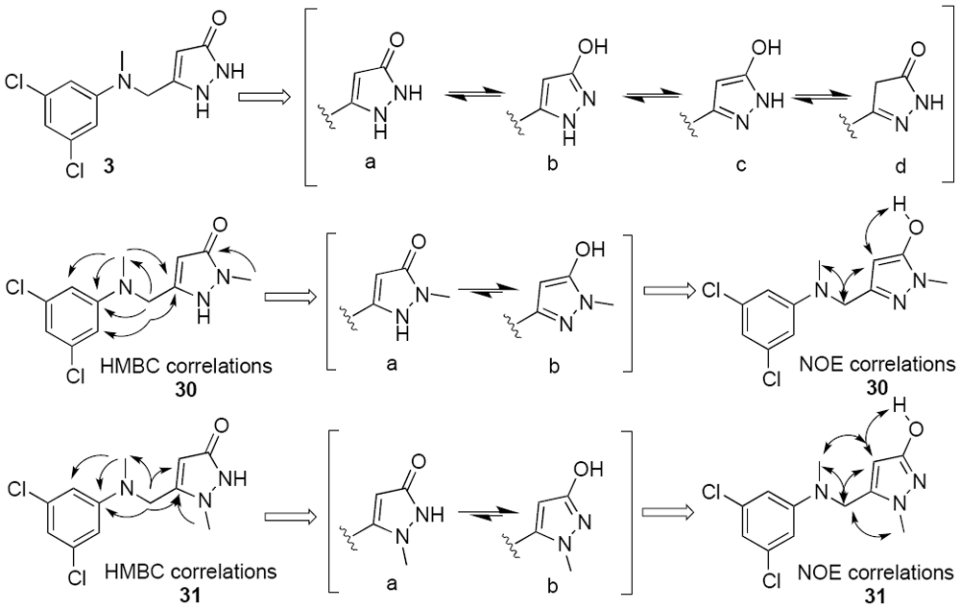

Figure 7.
Tautomerism, HMBC, and NOE spectral results of compounds **3, 30**, and **31**

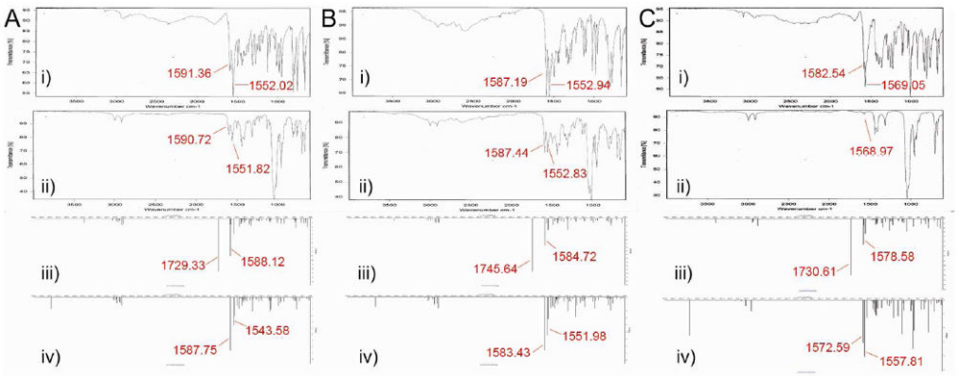

Figure 8.

Experimental and calculated IR spectral comparison: (A) compound **30**; (B) compound **31**; (C) compound **38**; i) experimental IR recorded in the solid phase; ii) experimental IR recorded in DMSO solution; iii) calculated IR of ketone-type tautomer (**30a**-like); iv) calculated IR of phenol-type tautomer (**30b**-like). The stretching vibrations of the C=O bond (~1730 cm^{-1}) and skeletal vibrations of the aromatic rings (1600~1550 cm^{-1}) are given in red.

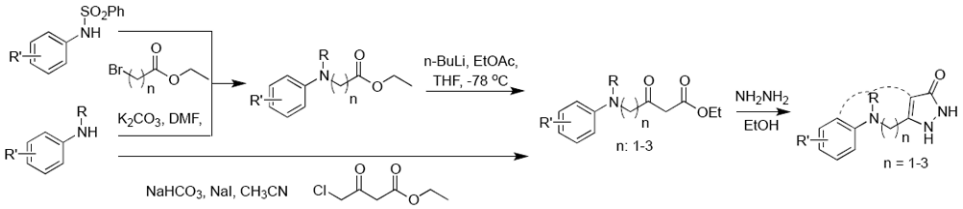

Scheme 1.
Synthetic routes for arylazanyl pyrazolones

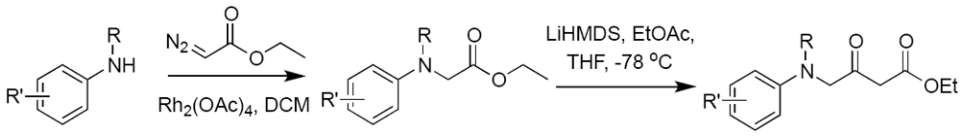

Scheme 2.
Synthesis of β-ketoester intermediates with bulky R groups

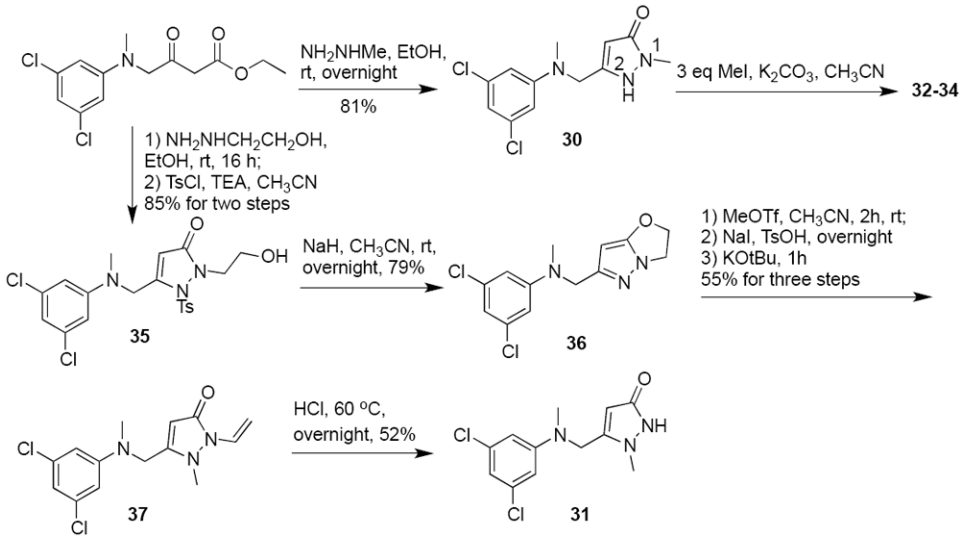

Scheme 3.
Synthesis of analogues substituted on the pyrazolone moiety

Table 1

In vitro microsomal stability of **1-3**[a]

		NADPH-dependent		NADPH-absent	
	Cmpd	**CL_{int}[b] (mL min^{-1} kg^{-1})**	**$T_{1/2}$[c] (min)**	**CL_{int}[b] (mL min^{-1} kg^{-1})**	**$T_{1/2}$[c] (min)**
Human	**1**	25	93	13	173
	2	24	95	0	>180
	3	0	>180	0	>180
Mouse	**1**	64	36	21	111
	2	78	30	23	100
	3	93	25	0	>180

[a]Data were obtained from Apredica.

[b]Microsomal intrinsic clearance.

[c]Half-life.

Table 2

In vitro Caco-2 permeability of **1-3**[a].

Cmpd	P_{app} (A→B)[b] (10^{-6} cm/s)	P_{app} (B→A)[b] (10^{-6} cm/s)	Efflux ratio (B→A)/ (A→B)
1	36.7	14.1	0.4
2	0.6	28.1	47.1
3	2.2	7.6	3.5

[a]Data were obtained from Apredica.

[b]Apparent permeability.

Table 3

Calculated energies of the tautomers of **3**

Tautomers	Energy (a.u.)	ΔE (kJ/mol)
3a	-1585.125802	22.60
3b	-1585.129852	11.97
3c	-1585.128450	15.64
3d	-1585.134409	0